

# Size and Volume Effects on the Strength of Microscale Lead-Free Solder Joints

L.M. YIN,<sup>1</sup> X.P. ZHANG,<sup>1,3</sup> and CHUNSHENG LU<sup>2</sup>

1.—School of Materials Science and Engineering, South China University of Technology, Guangzhou 510640, China. 2.—Department of Mechanical Engineering, Curtin University of Technology, Perth, WA 6845, Australia. 3.—e-mail: mexzhang@scut.edu.cn

The fracture behavior of microscale lead-free Sn-3.0Ag-0.5Cu solder joints of different sizes was investigated under quasistatic microtension loading. The experimental results show that the ultimate tensile strength of a joint does not always increase with decreasing thickness-to-diameter ratio ( $d/t$ ), which is commonly regarded as the dominant factor for mechanical constraint in the joint. A clear joint volume effect on the strength has been found, i.e., the joint's strength increases with decreasing joint volume ( $V = \frac{\pi}{4}d^2t$ ), and the correlation follows an inverse proportional function reasonably well.

**Key words:** Lead-free solder, volume effect, strength, mechanical constraint, intermetallic compounds

## INTRODUCTION

With the miniaturization of modern electronic products and devices, the packaging density of components such as chips significantly increases, and the scale of interconnections becomes smaller and smaller.<sup>1–3</sup> Consequently, the requirements for high integrity and reliability have demanded superior mechanical properties of interconnect materials, in which solder alloys play key roles. This is particularly true for lead-free solders which have poor process performance and lower integrity level compared with eutectic or near-eutectic tin-lead solders. As is well known, the properties of solder joints are very different from those of bulk solders. However, the properties of bulk solders have usually been used for solder selection and joint design, as well as for reliability estimation of electronic packages. Undoubtedly, this may lead to an inaccurate evaluation.

It has been shown that the material property data obtained from bulk solders are no longer reliable for reliability estimation of soldered interconnections in electronic packages when the volume of a solder is smaller than  $10^{-3}$  mm<sup>3</sup>, being nearly equivalent to a joint of 110  $\mu$ m in diameter and thickness.<sup>2,3</sup>

In addition, it is worth noticing that the performance of a solder joint is strongly dependent on its size. In contrast to the increasing concern about integrity and reliability of lead-free solder interconnections, there is not a good understanding of the effect of size on the mechanical behavior of microscale joints. In this communication, we report the strength and fracture behavior of microscale lead-free solder joints of different sizes (200  $\mu$ m to 575  $\mu$ m in diameter and 75  $\mu$ m to 525  $\mu$ m in thickness), and in particular a solder joint volume effect on the strength of mechanically constrained solder joints.

## EXPERIMENTAL PROCEDURES

Solder joints with a typical copper wire/solder/copper wire sandwich structure<sup>4</sup> were prepared with different sizes in this study. High-purity oxygen-free copper wires with diameters of 225  $\mu$ m, 300  $\mu$ m, 425  $\mu$ m, 500  $\mu$ m, and 600  $\mu$ m, and the lead-free solder Sn-3.0Ag-0.5Cu were used in joint samples, while Sn-37Pb solder was used for a comparative study. All solder joints were prepared by modeling the thermal cycle of the reflow process. A specially designed aluminum fixture with microscale V-grooves on its surface was made to assemble the solder joints. The thickness of the solder joints was designed to be 75  $\mu$ m, 125  $\mu$ m, 150  $\mu$ m, 175  $\mu$ m, 225  $\mu$ m, 325  $\mu$ m, 425  $\mu$ m, and 525  $\mu$ m. In soldering,

(Received January 4, 2009; accepted June 1, 2009; published online June 25, 2009)

copper wires and solder particles/balls were kept in flux (rosin-ethanol solution for Sn-37Pb solder and mildly activated rosin-ethanol solution for Sn-3.0Ag-0.5Cu solder), and the fixture was heated on a hot plate (1.5 kW). The typical soldering process for Sn-3.0Ag-0.5Cu solder was as follows: first, the hot plate was heated to 270°C; then the aluminum fixture (with the assembled joint pieces on it) was placed on the hot plate and heated to 250°C (i.e., the measured temperature at the joint sample or the fixture) at a heating rate of  $\sim 3^\circ\text{C/s}$ ; the assembled sample was kept at  $\sim 250^\circ\text{C}$  for  $\sim 20$  s; finally the fixture was quickly moved away from the hot plate and cooled by using a small electrical blower. The actual heating profile measured during the soldering process is shown in Fig. 1. In our studies, by using the above soldering process, more than 700 solder joints have been prepared with excellent repetition. After soldering, the joint samples were polished to diameters of 200  $\mu\text{m}$ , 275  $\mu\text{m}$ , 400  $\mu\text{m}$ , 475  $\mu\text{m}$ , and 575  $\mu\text{m}$ . Figure 2 shows a typical copper/Sn-3.0Ag-0.5Cu/copper sandwich structured joint with a thickness of 225  $\mu\text{m}$  and a diameter as small as 200  $\mu\text{m}$ , compared with 300  $\mu\text{m}$  used by Ren et al.<sup>4</sup> Uniaxial tension tests were conducted by using a dynamic mechanical analyzer (DMA Q800, TA-Instruments) at 35°C with a loading rate of 1 N/min.

## RESULTS AND DISCUSSION

As shown in Fig. 3a–c, the joint strength increases with decreasing thickness of the solder joint, and the strength of these joints is higher than that of bulk solders (45 MPa for Sn-3.0Ag-0.5Cu, 35 MPa for Sn-37Pb bulk solders<sup>5,6</sup>) and the evaluation by the Orowan approximation equation in the form  $\sigma_j = \sigma_{\text{UTS}} \left(1 + \frac{d}{6t}\right)$ ,<sup>3,7,8</sup> where  $\sigma_j$  is the tensile strength of the joint,  $\sigma_{\text{UTS}}$  is the ultimate tensile strength of the bulk solder, and  $d$  and  $t$  are the diameter and

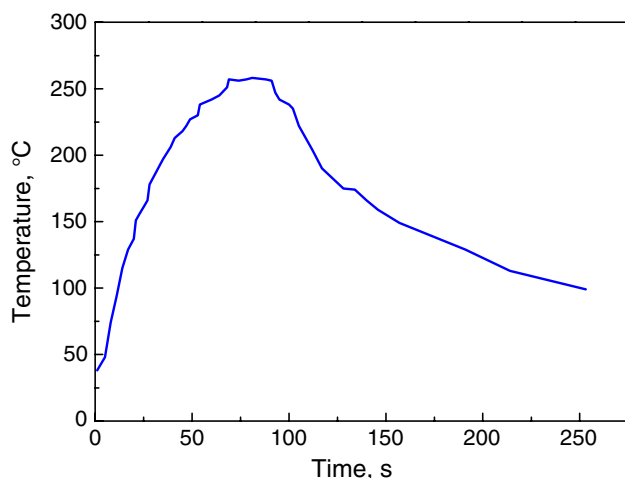


Fig. 1. Actual heating profile measured during the soldering process (Sn-3.0Ag-0.5Cu).

thickness of the joint, respectively. The increase of joint strength is mainly due to constraint strengthening induced by high triaxial stresses at the copper–solder interfaces of the joint. Since copper has a lower Poisson’s ratio ( $\sim 0.3$ ) and a higher Young’s modulus ( $\sim 120$  GPa) relative to Sn-Ag-Cu solder ( $\sim 0.4$  GPa and  $\sim 50$  GPa, respectively), the deformation mismatch between the “soft” solder part and the “hard” copper substrate leads to enhancement of the mechanical constraint effect and finally results in an increase in the strength of the solder joint.

However, the increase of the diameter of solder joints with constant thickness (e.g., 125  $\mu\text{m}$ , 225  $\mu\text{m}$ , and 325  $\mu\text{m}$ ) brings about a decrease of their strength (Fig. 3a, b, d); that is, the decrease of the thickness-to-diameter ratio of a joint results in a decrease of the joint tensile strength, which may be called an opposite size effect, i.e., the joint strength does not always increase with increasing mechanical constraint of the joint. Here the high level of interface stresses developed in a joint with small thickness-to-diameter ratio results in brittle fracture through intermetallic compound (IMC) layers along the joint interfaces. Although the localized high stress triaxiality leads to strengthening of the solder joint, it also induces high interface stresses. Thus, the joint strength depends on the combined action of both stress triaxiality and the interface stress state of the joint. In addition, the microstructures of the solder joints of different sizes (or volumes) were inspected by employing an optical microscope (Leica DM2500P). No obvious differences in microstructure in terms of phase constituents and grain size were observed for these solder joints.

As discussed above, the interfacial stress  $\sigma_r$  develops at the solder/copper interfaces owing to the occurrence of a change to a triaxial stress state from the initial uniaxial stress state, as shown in Fig. 4. The lower the joint thickness-to-diameter ratio  $t/d$ ,

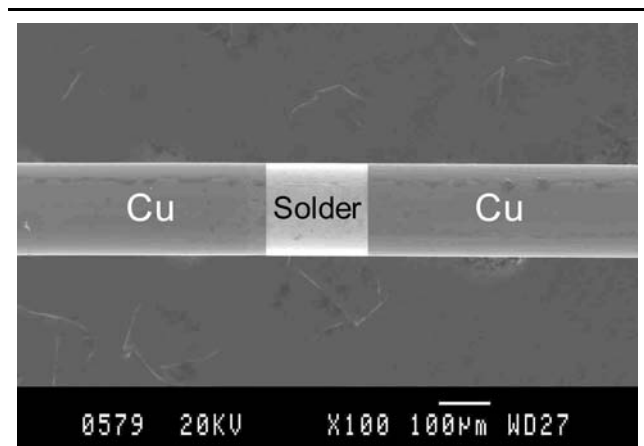


Fig. 2. SEM observation of a Cu/solder/Cu sandwich-structured solder joint with a diameter of 200  $\mu\text{m}$  and a thickness of 225  $\mu\text{m}$ .

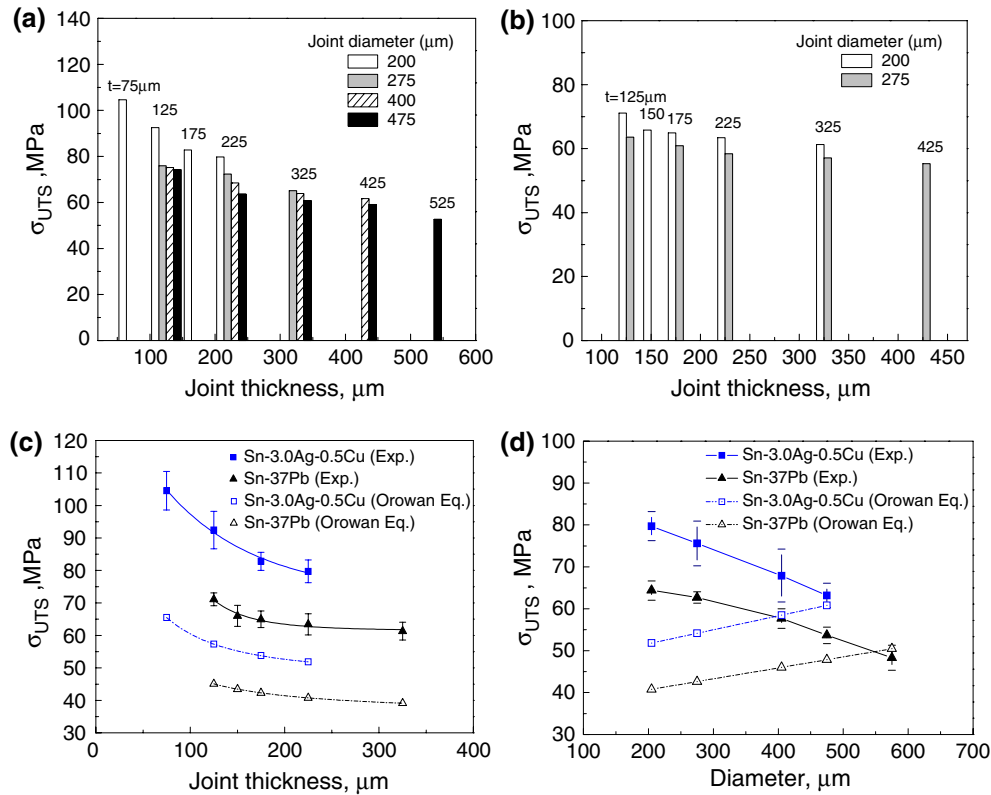


Fig. 3. Tensile strength of joints with different joint sizes: (a) distribution of the average tensile strength of Sn-3.0Ag-0.5Cu solder joints, (b) distribution of the average tensile strength of Sn-37Pb solder joints, (c) tensile strength versus joint thickness, and (d) tensile strength versus joint diameter.

the greater the interfacial stress  $\sigma_r$ ,<sup>9</sup> and the maximum value of the interfacial stress can reach half the ultimate tensile strength of the solder,  $\sigma_{r\max} = \frac{\sigma_{UTS}}{2}$ .<sup>7</sup> In addition, the triaxial stress state can be described using Bridgman's theory,<sup>10</sup> and the maximum stress triaxiality in the joint can be estimated by

$$\frac{\sigma_m}{\sigma_{\text{eff}}} = \frac{1}{3} + \ln\left(1 + \frac{d}{2R}\right), \quad (1)$$

where  $\sigma_m$  is the average stress,  $\sigma_{\text{eff}}$  is the effective stress,  $d$  is the diameter of the minimum cross-sectional area, and  $R$  is the radius of the outer notch formed after deformation, as shown in Fig. 4. For a joint with a small thickness, the  $R$  value may be a constant regardless of the diameter of the joint. It is easy to see that, the smaller the diameter, the lower the stress triaxiality, and the interfacial stress  $\sigma_r$  follows the rule  $\sigma_{r1} > \sigma_{r2}$ , where  $\sigma_{r1}$  and  $\sigma_{r2}$  denote the interface stress of joints with large and small diameter, respectively. The high interface stress may trigger cracking in the IMC layers of the joint and result in brittle fracture along the joint interfaces.

To further clarify the opposite size effect on the strength of the solder joints, loading interruption

tests were performed for joints with two diameters of 200  $\mu\text{m}$  and 575  $\mu\text{m}$  but the same thickness of 225  $\mu\text{m}$ . The joints were loaded to the elastic limit (or yield point) and then unloaded. The morphologies of the loaded joints were observed by scanning electron microscope (SEM) (JEOL, JSM-5200; Fig. 5). Clearly, for joints with a small diameter, the solder part deforms plastically and no crack occurs. Fractography of the joint after final fracture shows a typical necking fracture mode and fracture position located in the middle part of the joint (Fig. 5b). However, for the joint with a large diameter (575  $\mu\text{m}$ ), accompanying the plastic deformation of the solder, cracks initiate, and grow along the interfaces (Fig. 5c), and the final fracture takes place at the interfaces or across the solder at an angle of 45° (Fig. 5d, e). High-magnification SEM observation of the joint microstructure shows crack initiation and growth through the IMC ( $\text{Cu}_6\text{Sn}_5$ ) layers along the joint interfaces (Fig. 6).

More importantly, based on the analysis of a large amount of data obtained in this study, a solder joint volume effect on the tensile strength has been found, that is, the strength of the solder joint increases with decreasing solder joint volume  $V$  ( $V = \frac{\pi}{4}d^2t$ ), and the correlation between  $\sigma_j$  and  $V$  can be well described by an inverse proportion

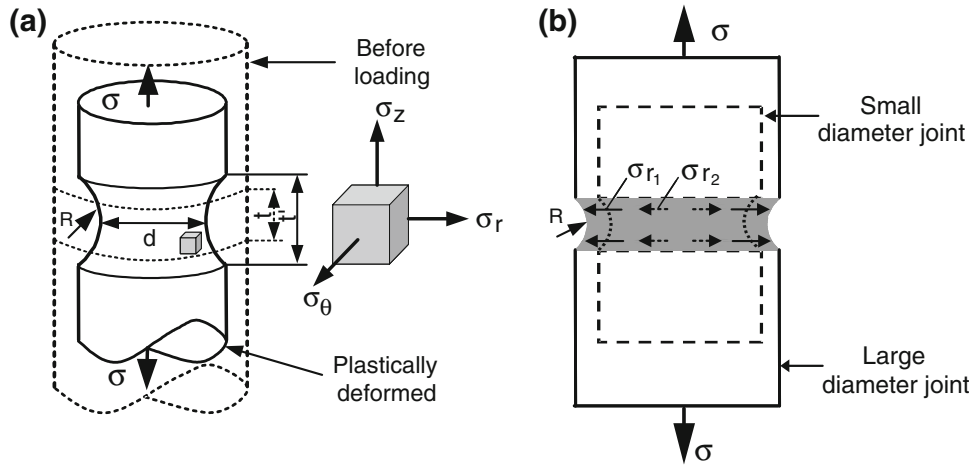


Fig. 4. Triaxial stress state and interface stresses in solder joints: (a) geometry of the joint and triaxial stresses after plastic deformation; (b) interface stresses developed.

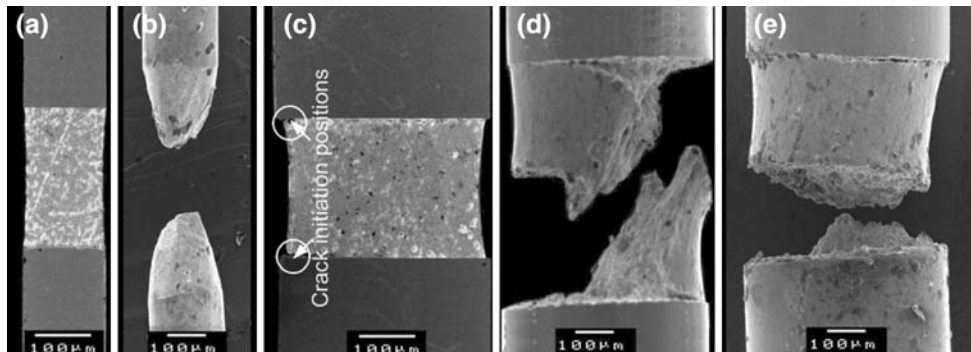


Fig. 5. Morphology of the joints with diameters of 200  $\mu\text{m}$  and 575  $\mu\text{m}$ , and the same thickness of 225  $\mu\text{m}$ : (a) after interruption test ( $d = 200 \mu\text{m}$ ), (b) after final fracture ( $d = 200 \mu\text{m}$ ), (c) after interruption test ( $d = 575 \mu\text{m}$ ), and (d, e) after final fracture ( $d = 575 \mu\text{m}$ ).

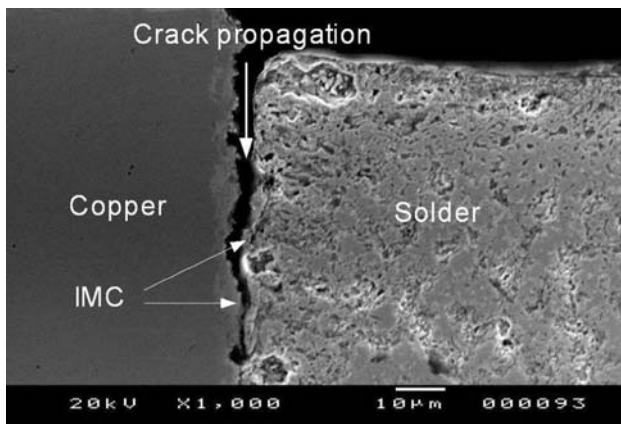


Fig. 6. High-magnification SEM observation of Fig. 5c shows crack initiation and growth in the IMC ( $\text{Cu}_6\text{Sn}_5$ ) layer along the interface of the joint.

function equation, i.e.,  $\sigma_j = \frac{1}{A_1 V} + B_1$  or  $\sigma_j = \frac{1}{A_2 d^{2t}} + B_2$ , (Fig. 7). For lead-free solder Sn-3.0Ag-0.5Cu microscale joints, the tensile strength can be estimated by  $\sigma_j = \frac{1}{6d^{2t}} + 59$ , or, for lead-containing

solder Sn-37Pb microscale joints:  $\sigma_j = \frac{1}{11d^{2t}} + 54$ . Clearly, the solder joint volume effect means that, the smaller the solder joint volume, the higher the joint strength.

## CONCLUSIONS

Two aspects of the size effects on the strength of the microscale solder joints are shown: the greatly increased strength over bulk solder, and the strong dependence upon the joint geometry and interface condition. The ultimate tensile strength of joints does not always increase with decreasing joint thickness-to-diameter ratio or increasing level of mechanical constraint effect. A clear solder joint volume effect on the strength exists, i.e., the joint's strength increases with decreasing solder joint volume and obeys an inverse proportion function: the smaller the joint volume, the higher the joint strength. For small joint thickness-to-diameter ratio, brittle fracture may occur at joint interfaces owing to the relatively high interfacial stresses, which lead to crack initiation and rapid growth in brittle intermetallic layers along the joint interfaces.

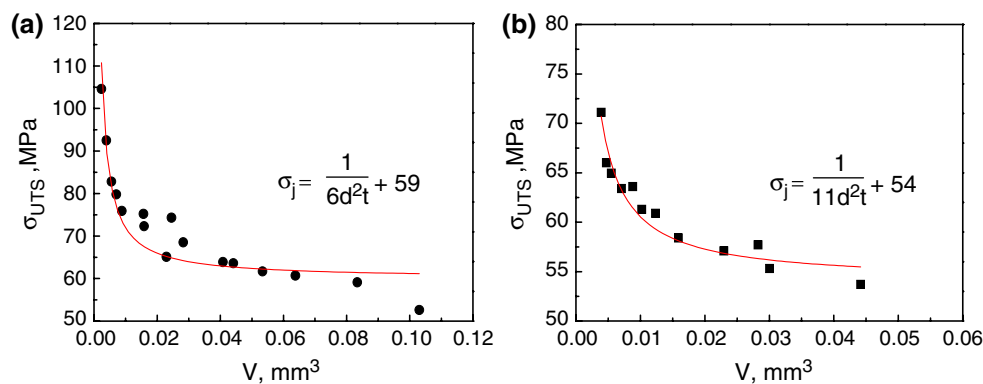


Fig. 7. Tensile strength versus solder joint volume: (a) Sn-3.0Ag-0.5Cu, and (b) Sn-37Pb.

### ACKNOWLEDGEMENTS

This research was supported by the Ministry of Education, China, through the NCET (04-0824) and its matching grant, and the Alexander von Humboldt Foundation through a grant of resumption of fellowship to XPZ (1037365). C.L. acknowledges support from the Curtin Internal Research Grant.

### REFERENCES

1. J. Cugnoni, J. Botsis, and J. Janczak-Rusch, *Adv. Eng. Mater.* 8, 184 (2006).
2. Z.H. Huang, P.P. Conway, E. Jung, R.C. Thomson, C.Q. Liu, T. Loeher, and M. Minkus, *J. Electron. Mater.* 36, 1761 (2006).
3. P. Zimprich, A. Betzwar-Kotas, G. Khatibi, B. Weiss, and H. Ipser, *J. Mater. Sci.: Mater. Electron.* 19, 383 (2008).
4. F. Ren, J.W. Nah, K.N. Tu, B. Xiong, L. Xu, and J.H.L. Pang, *Appl. Phys. Lett.* 89, 141914 (2006).
5. W.J. Plumbridge, *J. Mater. Sci.* 31, 2501 (1996).
6. K.S. Kim, S.H. Huh, and K. Suganuma, *Microelectron. Reliab.* 43, 259 (2003).
7. H.J. Saxton, A.J. West, and C.R. Barrett, *Metall. Trans.* 2, 999 (1971).
8. A.J. West, H.J. Saxton, A.S. Tetelman, and C.R. Barrett, *Metall. Trans.* 2, 1009 (1971).
9. T.H. Courtney, *Mechanical Behavior of Materials* (New York: McGraw Hill, 1990).
10. P.W. Bridgman, *Studies in Large Plastic Flow and Fracture* (Cambridge: Harvard University Press, 1964).